Electronic Supplementary Material (ESI) for Journal of Materials Chemistry C.

Supporting Information: Triplet-to-Singlet Exciton Transfer in Hyperfluorescent OLED materials

Leonardo Evaristo de Sousa,[1] Larissa dos Santos Born,[2] Pedro Henrique de Oliveira Neto,[2] and Piotr de Silva[1, a)]

[1)]*Department of Energy Conversion and Storage, Technical University of Denmark, Anker Engelunds Vej 301, 2800 Kongens Lyngby, Denmark*

[2)]*Institute of Physics, University of Brasilia, Brazil*

[a)]Electronic mail: pdes@dtu.dk

I. CALCULATION DETAILS

A. Functional Tuning

Molecule	ω (bohr^{-1})
ACRSA	0.1439
TBPe	0.1388
ACRXTN	0.1563
TTPA	0.1262
PXZ-TRZ	0.1438
TBRb	0.1051
Tri-PXZ-TRZ	0.1188
DBP	0.1114

TABLE S1. Tuned values of the range separation parameter ω.

All electronic structure calculations were performed with the ωB97X-D functional and the 6-31G(d,p) basis set. The range separation parameter was tuned for each of the molecules, and the results are shown in Table S1.

B. Absorption, Fluorescence and Phosphorescence Spectra

All spectra were calculated using the nuclear ensemble approach[1]. A total of $N = 500$ geometries were sampled for each spectrum simulation from the following distribution

$$\rho(\vec{R},T) = \prod_{i=1}^{3N-6} \left(\frac{\mu_i \omega_i}{2\pi\hbar \sinh\left(\hbar\omega_i / k_b T\right)} \right) \times \exp\left(-\frac{\mu_i \omega_i}{\hbar} R_i^2 \tanh\left(\frac{\hbar\omega_i}{2k_b T} \right) \right), \tag{S1}$$

where $\vec{R}$ is a displacement, T is the temperature (set to 300 K), and k_b is the Boltzmann constant. In addition, μ_i and ω_i are the reduced mass and frequency of the ith normal mode, respectively.

For absorption spectra, the normal modes are calculated for the S_0 state, whereas for fluorescence and phosphorescence, they are taken from calculations in the S_1 and T_1 states, respectively.

For each sampled geometry, a single point TD-DFT calculation is performed, and the final spectra are obtained by averaging over results according to the following expressions for the absorption cross section ($\sigma(E)$) and the differential emission rate (I(E))[1,2]:

$$\sigma(E) = \frac{\pi e^2 \hbar}{2mc\varepsilon_0} \frac{1}{N} \sum_{k=i}^{N} f_i G(E - \Delta E_i, \sigma), \tag{S2}$$

$$I(E) = \frac{n^2}{3\pi\hbar^3 c^3 \varepsilon_0} \frac{1}{N} \sum_{k=1}^{N} M_i^2 \Delta E_i^3 G(E - \Delta E_i, \sigma). \tag{S3}$$

In these expressions, c is the speed of light, ε_0 is the vacuum permittivity, and e and m correspond to the electron's charge and mass, respectively. In addition, f is the oscillator strength of the transition, ΔE_i is the vertical transition energy and M_i is the transition dipole moment. The function $G(E - \Delta E_i, \sigma)$ is a normalized gaussian distribution with mean $E - \Delta E_i$ and standard deviation $\sigma = k_b T$.

For phosphorescence spectra, it is necessary to employ perturbation theory to calculate the appropriate transition dipole moments, which are given by[3]

$$M_\gamma^\beta = \sum_m \frac{\left\langle T_m^\beta | H_{SO} | S_0 \right\rangle}{E(S_0) - E(T_m)} \left\langle T_1^\beta | M_\gamma | T_m^\beta \right\rangle + \sum_m \frac{\left\langle S_m | H_{SO} | T_1^\beta \right\rangle}{E(T_1) - E(S_m)} \left\langle S_m | M_\gamma | S_0 \right\rangle, \tag{S4}$$

in which γ refers to the x,y, and z coordinates and β indexes the sublevels of the triplet states. The summations include ten singlet and ten triplet excited states and the total transition dipole moment is averaged over the triplet sublevels as

$$M_i^2 = \frac{1}{3} \sum_{\gamma,\beta} |M_\gamma^\beta|^2, \tag{S5}$$

C. Rate Calculations

To calculate Förster transfer rates, we employ a corrected version of the usual point-dipole approximation expression given by[4,5]

$$k_F = \frac{1}{\tau_{emi}} \left(\frac{R_F}{\alpha\mu + r} \right)^6 \tag{S6}$$

where R_F is the Förster radius of the transfer, τ_{emi} is the fluorescence lifetime (phosphorescence lifetime for triplet-to-singlet transfers), r is the intermolecular distance, and $\alpha\mu$ is the correction term for small distances in which α is a constant (1.15 e^{-1}, e being the charge of the electron), and μ is the molecule's transition dipole moment.

The Förster radius can be obtained from spectrum simulations by the following expression[6]

$$R_F{}^6 = \frac{9c^4\kappa^2\hbar^3\tau_{emi}}{8\pi}\int_0^\infty \frac{dE}{E^4} I_D(E)\sigma_A(E) \tag{S7}$$

where κ is the orientation factor (set to $2/3$ for isotropic distribution of dipoles), I_D is the donor molecule's differential emission rate (for fluorescence or phosphorescence), and σ_A is the acceptor's absorption cross section.

The radiative emission lifetime (τ_{emi}) for either fluorescence or phosphorescence can be obtained from the corresponding emission spectrum of the molecule and relates to the radiative emission rate k_{emi} by

$$k_{emi} = \frac{1}{\tau_{emi}} = \frac{1}{\hbar}\int_0^\infty I_D(E)dE \tag{S8}$$

Intersystem crossing (ISC) rates are calculated from the same ensemble of geometries used for spectrum simulations using the following expression[2]

$$k_{ISC} = \frac{2\pi}{\hbar}\frac{1}{N}\sum_{k=1}^{N} H_{SO_i}^2 G(\lambda + \Delta E_{fi}, \sqrt{2\lambda k_b T + \sigma^2}), \tag{S9}$$

in which H_{SO_i} is the spin-orbit coupling for the i-th sampled geometry and λ is the reorganization energy of the $S_1 \rightarrow T_1$ transition in the case of ISC and the $T_1 \rightarrow S_1$ transition in the case of reverse ISC (rISC). These reorganization energies are shown in Table S2

Molecule	Reorganization energy (eV)	
	$S_1 \rightarrow T_1$	$T_1 \rightarrow S_1$
ACRSA	0.189	0.118
ACRXTN	0.218	0.221
PXZ-TRZ	0.192	0.216
Tri-PXZ-TRZ	0.192	0.075

TABLE S2. Reorganization energies used to calculate ISC and rISC rates.

II. KINETIC MONTE CARLO DETAILS

Kinetic Monte Carlo simulations are run on a $50 \times 50 \times 50$ cubic lattice. Each site in the lattice is considered to be either a TADF molecule or a fluorescent emitter. Host molecules are not taken

Molecule	Molar mass (g/mol)
ACRSA	435.51
TBPe	476.73
ACRXTN	403.47
TTPA	568.75
PXZ-TRZ	490.55
TBRb	757.09
Tri-PXZ-TRZ	826.90
DBP	804.97

TABLE S3. Molar masses of all compounds analyzed in this work.

into account in the simulation since they do not participate in the processes of exciton transfer and emission. They are, however, accounted for in the estimation of intermolecular distances.

To determine intersite distances, we considered a box of volume V to contain n_1 TADF dopants, n_2 fluorescent emitters, and n_3 host molecules. The average distance between two molecules of either TADF or emitter kind is given by

$$d = \left[\frac{V}{(n_1+n_2)}\right]^{1/3} \tag{S10}$$

We consider further that the total volume can be given by $V = Nd_0^3$, in which $N = n_1+n_2+n_3$ is the total number of molecules and d_0^3 is an average volume occupied by each molecule. As such, we may write

$$d = d_0\left[\frac{N}{(n_1+n_2)}\right]^{1/3} \tag{S11}$$

The term in square brackets is the inverse of the fraction of TADF plus fluorescent emitters present in the box. This number can be connected to the weight fraction (p_i) of each compound i employed in the experimental setup and their corresponding molar masses (m_i), which are shown in Table II. This is given by

$$p_i = \frac{n_i m_i}{M} \Rightarrow n_i = \frac{p_i}{m_i}M \tag{S12}$$

in which M is the total mass of the box. From this follows that

System	ρ_1 (%)	ρ_2 (%)	d (Å)
ACRSA/TBPe	94.3	5.7	15.06
ACRXTN/TTPA	98.6	1.4	10.99
PXZ-TRZ/TBRb	97.5	2.5	13.86
Tri-PXZ-TRZ/DBP	93.6	6.4	18.90

TABLE S4. Fraction of lattice sites assigned as TADF and emitter molecules for weight fractions reported in Ref. 8 along with the corresponding estimated average intermolecular distances d_0.

$$\frac{(n_1+n_2)}{N} = \frac{\frac{p_1}{m_1}+\frac{p_2}{m_2}}{\frac{p_1}{m_1}+\frac{p_2}{m_2}+\frac{p_3}{m_3}} \tag{S13}$$

which allows calculation of d in Equation S11 once a d_0 value is chosen. To estimate this parameter, we have considered results from molecular dynamics simulations of mCP host molecules[7]. These simulations included 100 mCP molecules with a resulting density of 1 g cm^{-3}. This result gives an average intermolecular distance of 8.79 Å, which we use as our d_0 value.

Finally, to determine the fraction of lattice sites that will be considered as TADF molecules (ρ_1) or fluorescent emitters (ρ_2) we calculate

$$\rho_i = \frac{n_i}{(n_1+n_2)} = \frac{\frac{p_i}{m_i}}{\frac{p_1}{m_1}+\frac{p_2}{m_2}} \tag{S14}$$

For the weight fractions used in the experimental paper, the proportions of TADF and emitter molecules in the lattices are shown in Table S4.

III. SUPPORTING RESULTS

In this section, we present a series of supporting results from the various calculations performed. It includes a comparison between calculated and experimental absorption and emission energies, spectral overlap plots indicating the possibility of Förster transfers from emitters to TADF molecules and also between TADF molecules.

We also present tables with estimated fluorescence rates of the fluorescent emitters analyzed in this work, along with the Förster radii for singlet exciton transfers between emitters.

Molecule	Absorption (eV)		Fluorescence (eV)	
	Calc.	Exp.[8]	Calc.	Exp.[8]
ACRSA	3.04	-	2.91	2.55
TBPe	3.06	2.82	2.63	2.69
ACRXTN	2.91	-	2.81	2.53
TTPA	2.75	2.61	2.27	2.34
PXZ-TRZ	2.71	-	2.53	2.30
TBRb	2.42	2.38	2.03	2.18
Tri-PXZ-TRZ	2.45	-	2.40	2.27
DBP	2.32	2.10	1.94	2.03

TABLE S5. Comparison between calculated and experimental values for absorption and fluorescence energy peaks for all TADF/emitter pairs analyzed here.

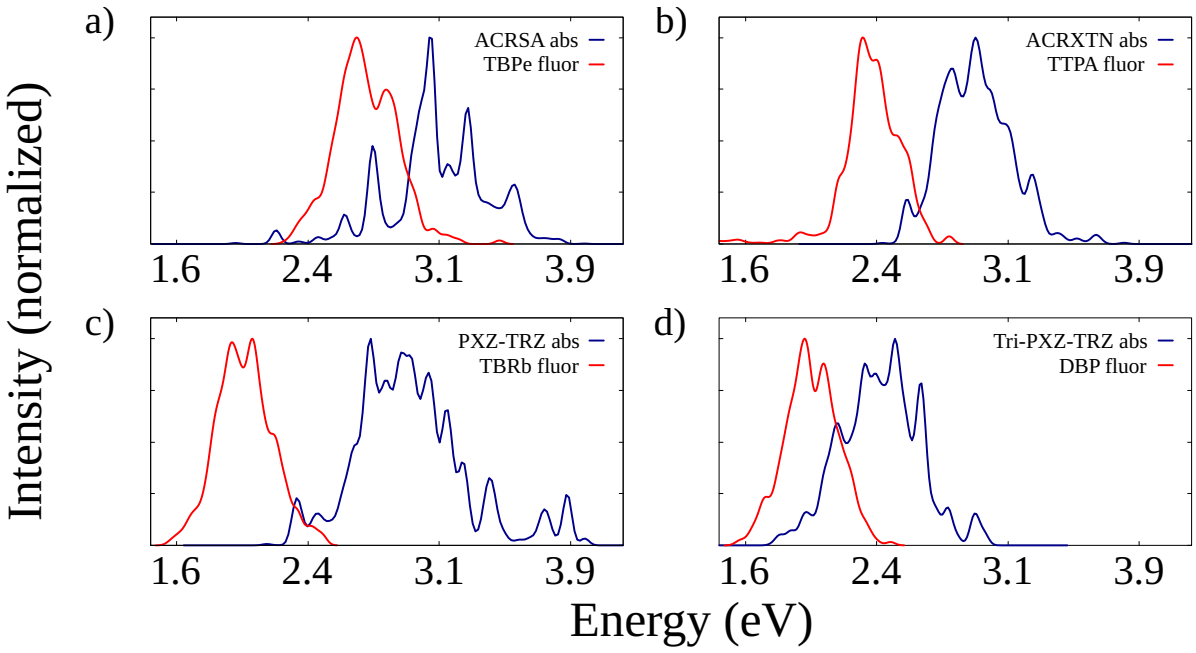

FIG. S1. Spectral overlaps between the fluorescence spectra of the fluorescent emitters and the absorption spectra of the TADF molecules they are paired with.

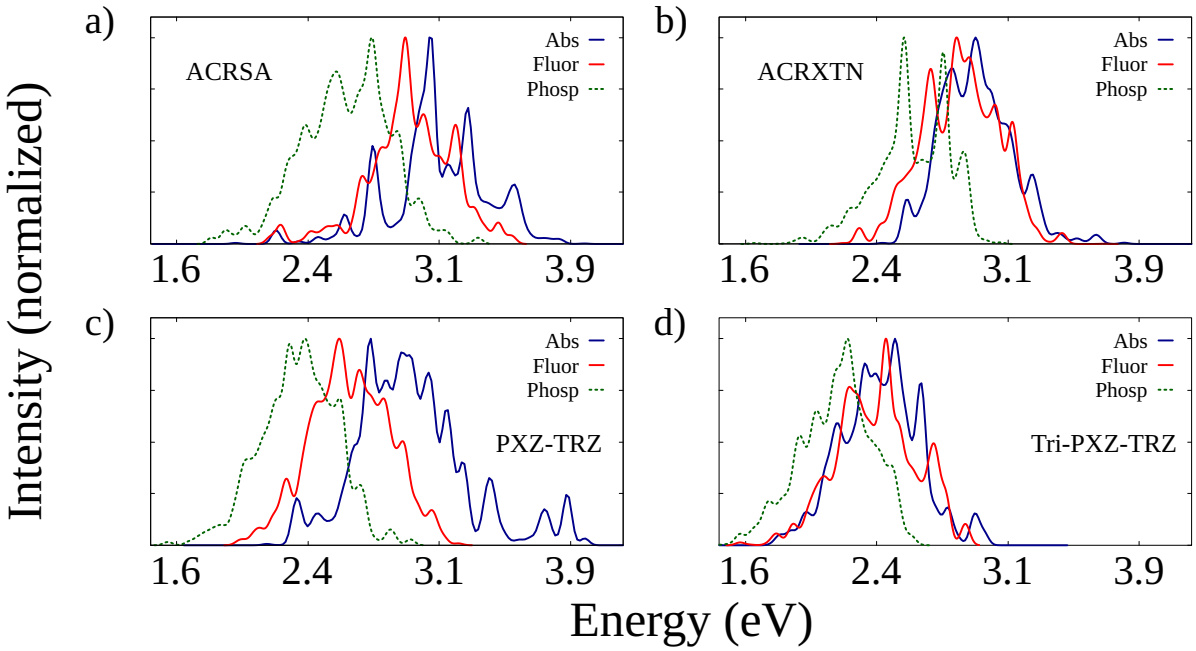

FIG. S2. Spectral overlaps between the fluorescence and phosphorescence spectra of the TADF molecules and their own absorption spectra.

Molecule	Förster radius (Å)
	$S_1 \rightarrow S_1$
TBPe	50.1
TTPA	37.5
TBRb	51.8
DBP	73.9

TABLE S6. Förster radii for singlet exciton transfers between different fluorescent emitters of the same kind.

Emitter	Fluor. (s^{-1})
TBPe	8.13×10^{8}
TTPA	6.66×10^{7}
TBRb	2.46×10^{8}
DBP	1.07×10^{9}

TABLE S7. Estimated fluorescence rates for the fluorescent emitters analyzed in this work.

System	$r_1 = \frac{\phi_{TTS}}{\phi_{rISC}\phi_{STS}}$		$r_2 = \frac{\phi_{TTS}}{\phi_{rISC}}$	
	$T_1^{TADF} \rightarrow S_1^{TADF}$	$T_1^{TADF} \rightarrow S_1^{EM}$	$T_1^{TADF} \rightarrow S_1^{TADF}$	$T_1^{TADF} \rightarrow S_1^{EM}$
ACRSA/TBPe	40.1	125.9	0.7	99.0
ACRXTN/TTPA	41.6	68.8	40.9	67.3
PXZ-TRZ/TBRb	1.3	56.3	1.2	56.2
Tri-PXZ-TRZ/DBP	0.0	1.2	0.0	1.2

TABLE S8. Ratios between the quantum yields of two processes that allow a triplet exciton to be transferred to a nearby molecule as a singlet (r_1): TTS and rISC followed by singlet-to-singlet (STS) FRET. On the right, ratios between the quantum yields of two triplet conversion mechanisms (r_2): TTS and rISC. The table shows the ratios for transfers between TADF molecules (superscript TADF) and from TADF to emitter molecules (superscript EM).

REFERENCES

[1]R. Crespo-Otero and M. Barbatti, "Spectrum simulation and decomposition with nuclear ensemble: formal derivation and application to benzene, furan and 2-phenylfuran," in *Marco Antonio Chaer Nascimento* (Springer, 2014) pp. 89–102.

[2]L. E. de Sousa and P. de Silva, "Unified framework for photophysical rate calculations in tadf molecules," Journal of Chemical Theory and Computation **17**, 5816–5824 (2021).

[3]B. Minaev, G. Baryshnikov, and H. Agren, "Principles of phosphorescent organic light emitting devices," Phys. Chem. Chem. Phys. **16**, 1719–1758 (2014).

[4]K. F. Wong, B. Bagchi, and P. J. Rossky, "Distance and orientation dependence of excitation transfer rates in conjugated systems: beyond the förster theory," The Journal of Physical Chemistry A **108**, 5752–5763 (2004).

[5]S. R. Yost, E. Hontz, S. Yeganeh, and T. Van Voorhis, "Triplet vs singlet energy transfer in organic semiconductors: the tortoise and the hare," The Journal of Physical Chemistry C **116**, 17369–17377 (2012).

[6]S. Lin, C. Chang, K. Liang, R. Chang, J. Zhang, T. Yang, M. Hayashi, Y. Shiu, and F. Hsu, "Ultrafast dynamics and spectroscopy of bacterial photosynthetic reaction centers," Advances in chemical physics **121**, 1–88 (2002).

[7]F. Suzuki, K. Shizu, H. Kawaguchi, S. Furukawa, T. Sato, K. Tanaka, and H. Kaji, "Multiscale simulation of charge transport in a host material, n, n'-dicarbazole-3, 5-benzene (mcp), for organic light-emitting diodes," Journal of Materials Chemistry C **3**, 5549–5555 (2015).

[8]H. Nakanotani, T. Higuchi, T. Furukawa, K. Masui, K. Morimoto, M. Numata, H. Tanaka, Y. Sagara, T. Yasuda, and C. Adachi, "High-efficiency organic light-emitting diodes with fluorescent emitters," Nature communications **5**, 1–7 (2014).